Microfluid Nanofluid (2010) 9:1143–1149
DOI 10.1007/s10404-010-0635-y

RESEARCH PAPER

Improved performance of deterministic lateral displacement arrays with triangular posts

Kevin Loutherback · Kevin S. Chou · Jonathan Newman · Jason Puchalla · Robert H. Austin · James C. Sturm

Received: 17 February 2010 / Accepted: 22 April 2010 / Published online: 21 May 2010

Abstract Deterministic lateral displacement arrays have shown great promise for size-based particle analysis and purification in medicine and biology. Here, we demonstrate that the use of an array of triangular rather than circular posts significantly enhances the performance of these devices by reducing clogging, lowering hydrostatic pressure requirements, and increasing the range of displacement characteristics. Experimental data and theoretical models are presented to create a compelling argument that future designs of deterministic lateral displacement arrays should employ triangular posts. The effect of practical considerations, such as vertex rounding, post size, and shape, is also discussed.

Keywords Lateral displacement · Particle separation · Throughput · Clogging · Triangular posts

1 Introduction

A key step in many analytical and preparative techniques in medicine and biology is to separate cells, functionalized beads, or other particles from a solution which may contain other undesirable elements (Squires and Quake 2005; Pamme 2007; Yi et al. 2006; Rida and Gijs 2004; Lu et al. 2004). Deterministic lateral displacement, a size-based particle sorting method, has shown extremely high size selectivity, adaptability to sorting multiple particle sizes (Huang et al. 2004), dynamic control of critical particle sizes (Beech and Tegenfeldt 2008), and a broad range of operating conditions, sorting particles from 100 nm (Morton et al. 2006) to 30 μm (Davis et al. 2006). However, several limitations hinder the broader applicability of this technique. The sorting mechanism relies on particles being physically displaced by an array of posts, with the open space between posts on the same order as the critical sorting size. As a result, there is a maximum particle size that an array can accept without clogging, requiring multiple separation stages if the input sample has a broad distribution of particle sizes (Davis et al. 2006). Furthermore, the small gaps between the posts can lead to a large pressure drop across the device for a reasonable throughput compared to competing methods that rely on inertial effects and have much larger feature sizes (Di Carlo et al. 2007; Bhagat et al. 2008). Recent work by the Tegenfeldt group showed that the dynamic range of DLD arrays could be increased using dielectrophoretic effects (Beech et al. 2009), but this work will rely only on hydrodynamic effects resulting from the post geometry.

We recently reported that changing the post shape can result in two distinct critical particle sizes by changing the shape of the flow profile through the gap (Loutherback et al. 2009). By changing the posts from the usual circular to triangular shape, an asymmetry is created in the flow profile through the gap that shifts fluid flux toward the triangle vertex. This results in direction dependent critical particle sizes. For example, as the particles in Fig. 1 move left to right, they will be displaced by the vertex of the

K. Loutherback (✉) · R. H. Austin · J. C. Sturm
Princeton Institute for the Science and Technology of Materials (PRISM), Princeton University, Princeton, NJ, USA
e-mail: klouther@princeton.edu

K. Loutherback · K. S. Chou · J. Newman · J. C. Sturm
Department of Electrical Engineering, Princeton University, Princeton, NJ, USA

J. Puchalla · R. H. Austin
Department of Physics, Princeton University, Princeton, NJ, USA

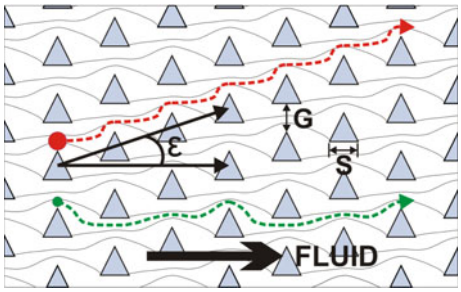

Fig. 1 Deterministic lateral displacement array with relevant parameters and features. The array is composed of columns of triangular posts of side length S with gap G between posts that are offset some small amount with respect to the direction of bulk fluid flow to produce array axis tilted an angle ε with respect to the fluid flow. Fluid flowing through gaps can be partitioned into $1/\varepsilon$ streams delineated by stagnation streamlines, each carrying equal volumetric flux. Particles in the fluid exhibit one of two behaviors depending on their size relative to the width of stream adjacent to the post as they move through a gap. Particles whose radii are narrower will follow streamlines in the fluid flow, denoted by the green particle with dotted trajectory, and remain bound within one stream as they move through the array. Particles whose radii are larger than the stream width, denoted by the red particle with dotted trajectory, cannot fit within the stream adjacent to the post as they travel through a gap and will be displaced into the adjacent stream. This occurs at each column of posts and the particle travels along the array axis at an angle ε with respect to the fluid flow. The critical particle diameter for the onset of this displacement is thus twice the width of the stream adjacent to the top of the post. As shown in (Loutherback et al. 2009), using triangular posts results in different critical size depending on which side of the post displaces the particle, with the critical size for being displaced by the vertex smaller than for the flat edge. Left to right fluid motion in this figure results in displacement by the vertex

triangle and the critical size will be the stream width just above the vertex. However, if the flow is reversed, then they will be displaced by the flat edge of the triangle and the critical size will be the stream width just below the triangle edge. Particles whose size falls between these two critical sizes will undergo a net displacement orthogonal to the flow after one cycle of flow direction while particles outside of this range will show no net displacement. As a result, we showed that particles in the intermediate range can be separated from other particles in an oscillating flow (Loutherback et al. 2009). The shift in flux toward the vertex of the triangle also leads to a compressed stream width along this edge and hence reduced critical particle size compared to a similar array with circular posts. This compression is central to the improvements that will be discussed in this article. We previously showed how the shifted flow profile created by triangular posts could be used to create a deterministic microfluidic ratchet with an oscillating flow (Loutherback et al. 2009). However, in this study, we discuss additional improvements in particle separation enabled by changing the post shape including reduced clogging and lower hydrostatic pressure requirements (Table 1).

Table 1 Critical particle sizes normalized to gap height for arrays with triangular posts and circular posts for various array tilts

Tilt angle	Critical size/ gap (triangle)	Critical size/ gap (circle)
1/5	0.45	0.56
1/6	0.39	0.50
1/8	0.32	0.43
1/10	0.28	0.38
1/12	0.24	0.34
1/15	0.21	0.30
1/20	0.17	0.26
1/30	0.13	0.21
1/50	0.09	0.16
1/100	0.06	0.11

2 Methods

The findings presented here are a result of both numerical simulations and experimental study. Comparisons between various post shapes were made using numerical simulation. Arrays similar to those shown in Fig. 1 were modeled by solution of the 2D incompressible Navier–Stokes equation in finite-element solver COMSOL Multiphysics. Flow profiles were extracted from a heavily meshed region between posts to calculate the critical particle size as in Inglis et al. (2006). Simulations were supplemented by experiments to confirm the predicted critical particle size for triangular posts and to compare the throughput between arrays with circular and triangular posts.

Experiments were conducted by observing the behavior of fluorescent polystyrene beads (Duke Scientific, Waltham, USA) in arrays fabricated in silicon. Samples were etched to a depth between 10 and 20 μm using an STS ASE Multiplex tool (Newport, UK), and through-wafer sandblasting was used to create inlet holes using 50-μm aluminum oxide particles (Danville Engineering, San Ramon, USA). Devices were sealed with a thin PDMS film fixed to a glass coverslip backplane and mounted to an acrylic jig connected to an external vacuum pump. Differential air pressure was used to control fluid flow through the chip. Particle motion was recorded as video with an EMCCD camera (QImaging, Surrey, Canada) at 10 fps, and pressure gradients were measured with a manometer (Sper Scientific, Scottsdale, USA).

3 Results and discussion

Triangular posts introduce a shifted rather than symmetric parabolic flow profile across the gap in deterministic lateral displacement arrays. Figure 2a and b shows numerically

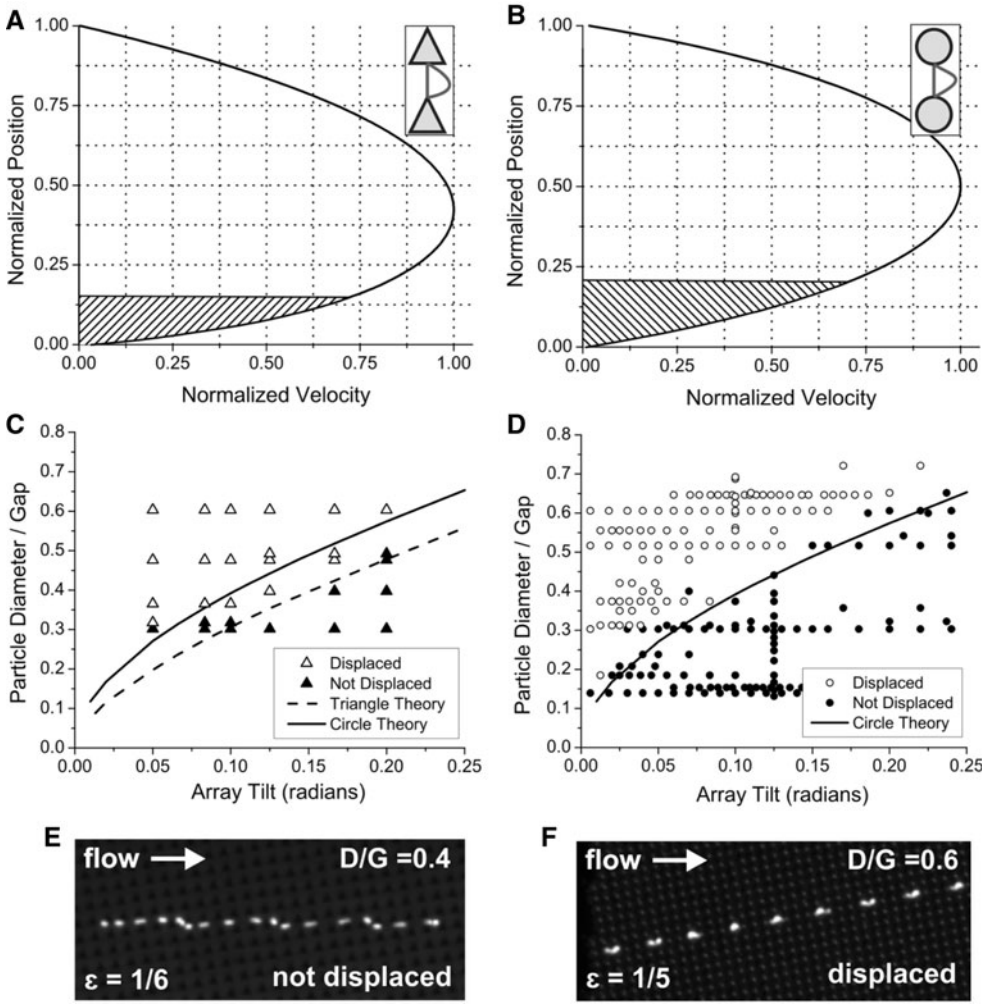

Fig. 2 **a**, **b** Numerically simulated flow profiles for arrays with triangular (**a**) and circular (**b**) posts. Fluid flowing in stream adjacent to bottom post for array with tilt 1/10 has been plotted to emphasize the effect of shifted flow profile that results from triangular posts. Post orientation shown in *inset*. **c**, **d** Experimentally observed behavior of fluorescent beads compared to theoretical prediction of critical particle size for triangular (**c**) and circular (**d**) posts. Observed particles, represented *triangles* and *circle*, are open if they were displaced by the array and closed if they were not displaced by the array. Theoretically predicted behavior is denoted by the *dotted* (triangular) and *solid* (circular) lines. Both theoretical critical size lines are plotted in (**c**) to emphasize the reduction enabled by triangular posts. Data for **d** adapted from (Inglis et al. 2006) with additional data points added. **f**, **e** Bead trajectories used to compile (**c**). **f** shows the trajectory of a 2.5-μm bead that is not displaced by an array with 6.3 μm gap and 1/6 tilt angle. **e** shows the trajectory of a 3.8-μm bead that is displaced by an array with 6.3-μm gap and 1/5 tilt angle

simulated flow profiles across the gaps in arrays with circular and triangular posts. Both flow profiles are normalized to the width of the gap between posts and the maximum velocity. The fluid constituting the first stream for tilt angle $\varepsilon = 1/10$, representing 10% of the total flow through the gap, has been shaded to emphasize the reduction in stream width. The first stream decreases from 20%, of the gap with the circular posts, to 15%, of the gap with the triangular posts, resulting in a smaller critical particle size as a ratio of the gap when using triangular posts. The critical particle size in these arrays can be estimated using the method described by Inglis et al. (2006). In brief, this method says the width of the first stream adjacent to a post is found by integrating over the velocity profile from a post edge until the area under the curve contains ε times the total area under the curve. While the results in Inglis et al. (2006) focused on two simple flow profiles (parabolic for hydrodynamic flow and plug for electroosmotic flow), the method they proposed can be generalized to any flow profile to predict the critical particle size in arrays with different post shapes. Predictions for the profiles in Fig. 2a and b are plotted as solid and dashed lines for circular and triangular posts, respectively, in Fig. 2c and d along with observed behavior (displaced or not displaced) of fluorescent beads of various sizes as a function of array tilt. Fluorescent beads with diameters

ranging from 1.9 to 3.8 μm were used to characterize the behavior of particles in arrays with 4.7-μm posts, 6.3-μm gaps, and various tilt angles. Obstacles were placed in a larger channel 3.4 mm wide and 16.8 mm long that maintains the tilt angle between the array axis and direction of bulk flow. Fluid motion is driven by applied pressure of a hand-operated syringe. Between 5 and 10 particles were observed at each size and tilt to determine characteristic behavior. Examples of these behaviors are shown in Fig. 2e and f. The Reynolds number was $\sim 10^{-4}$ for $L \sim 1$ μm, $V \sim 100$ μm/s and the Peclet number was ~ 100 for $D \sim 1$ μm^2/s from Einstein relation for diffusion coefficient of a spherical particle; therefore, effects of flow velocity and particle diffusion should not affect these observations. Particles above the line should be displaced by the array while those below the line should not. The theoretical predictions seem to set a lower bound on the size of a particle that will be displaced in the array. Notice that no displaced particles (open triangles in Fig. 2c or open circles in Fig. 2d) are seen below the predicted line for each post.

Predicted critical particle size as a function of array tilt for both circular and triangular posts has been plotted in Fig. 2c to emphasize how changing the post shape reduces the critical particle size as a ratio of the gap. For any practical tilt angle (ε between 1/5 and 1/100), the critical size in an array with triangular posts is substantially smaller than a similar array with circular posts, up to 10% of the gap for the steeper tilt angles. There are three ways to take advantage of this effect. First, for the same gap and tilt, an array using triangular posts can separate smaller particles. Second, for the same critical particle size and gap, the tilt of the array can be increased, reducing the overall length of the array and providing a small increase in throughput for a given applied pressure. The third and most important improvement is to allow an expansion of the gap while achieving the same critical particle size and array tilt. It is this last improvement that leads to both reduced array clogging and higher throughput.

3.1 Reduced clogging

Particles larger than the gap will clog the array. Biological samples often contain a broad range of particles with various sizes; therefore, multiple separation stages are sometimes necessary to ensure that the array continues to function (Davis et al. 2006). Using triangular posts allows one to increase the size of the gap for a given critical particle size and reduce the chances that the array will clog. Figure 3 shows the ratio of triangular gap size G_T to the circular gap size G_C for fixed critical particle size as a function of array tilt. In the practical range of array tilt from 1/100 to 1/5, the ratio scales from 1.94 to 1.27.

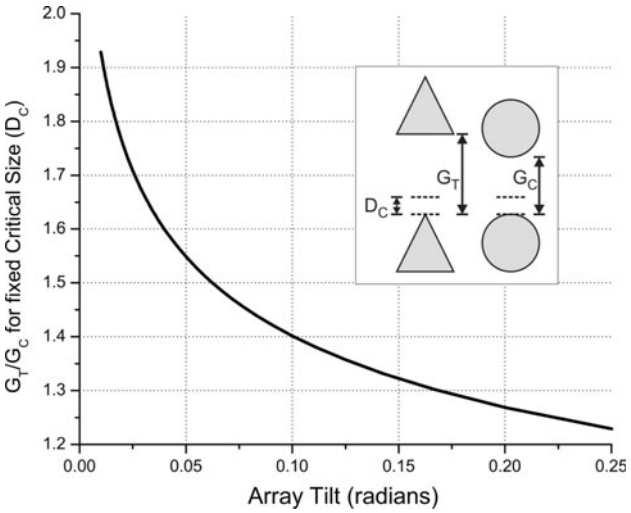

Fig. 3 Ratio of gaps for triangular (G_T) and circular (G_C) post arrays for fixed critical particle size as a function of array tilt

3.2 Increased throughput

The larger gap enabled by triangular posts allows an increase in flow rate (or separation throughput) for a given pressure gradient. This was confirmed experimentally by measuring average velocity of beads in two similar arrays. Two arrays with were constructed with nearly identical characteristics and triangular or circular posts. They each had the same overall channel width (5 mm) and length (20 mm), depth (20 μm), tilt (1/10), and critical particle size of 3.2 μm. One array had circular posts with diameter 6 μm with a gap of 8.3 μm and the second had equilateral triangular posts arranged as in Fig. 1 with side length 6 μm and gap 10.5 μm. The trajectories of 500-nm fluorescent beads were recorded with an EMCCD camera capturing video at 10 fps and then analyzed in MATLAB for various pressure gradients across the array. Pressure gradients were varied with a bleeder valve attached to a vacuum pump and measured with manometer attached in line with the pump. Small particles that would not be displaced by the array were chosen so they would sample each of the flow streams evenly and provide an accurate representation of the average fluid velocity (Lindken et al. 2009). Bead trajectories were isolated, and an average velocity for each bead was determined by averaging its instantaneous velocity as it traversed several periods of the array. These values were then averaged together to produce an overall average bead velocity for a given pressure drop across the array. Between 4 and 19 beads with an average of 10.5 beads were tracked for each data point. The average particle velocities are plotted in Fig. 4 as a function of pressure drop along with a weighted least squares fit for each array. Comparing the slopes of the two linear fits, it can be seen that particles in the array with triangular posts travelled 85 ± 10% faster on average than those in an array

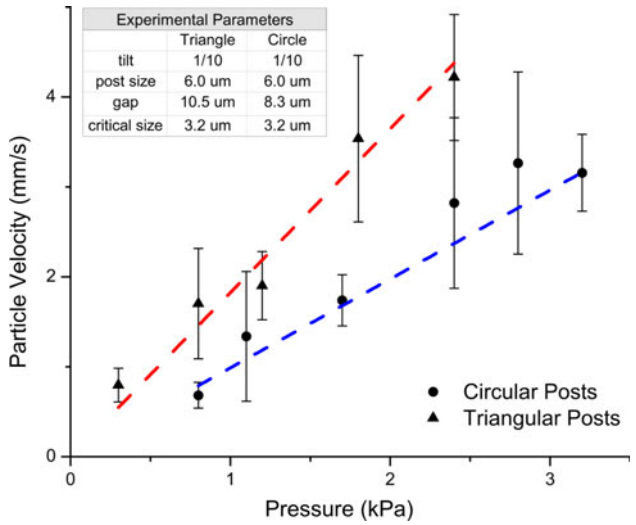

Fig. 4 Experimental throughput comparison of arrays with triangular and circular posts. The average velocities of beads that were not displaced by the array are plotted as a function of pressure drop along with a linear fit for each array. The average particle velocity for the same pressure gradient is 85% faster in an array with triangular posts than circular posts

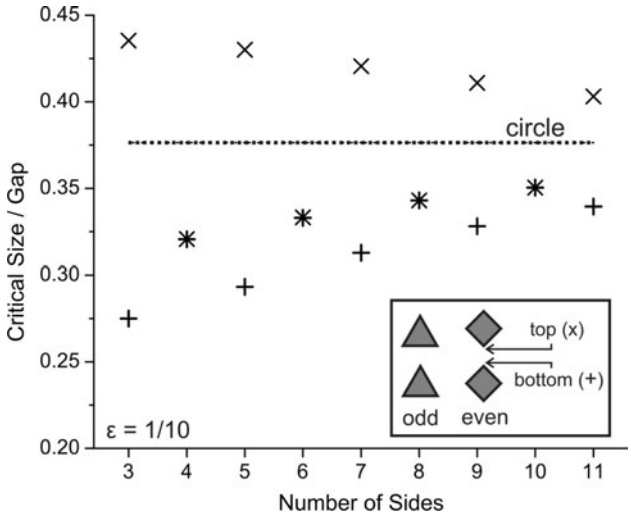

Fig. 5 Critical particle size for arrays with regular polygon posts with varying number of sides. Arrays consist of posts with 10 μm altitude with 10 μm gap. Numerically simulated flow profiles across each gap were extracted from flow field simulations and critical particle size plotted for both top and bottom of post for array tilt $\varepsilon = 1/10$ with critical particle size for circular posts plotted as a dotted line for reference

with circular posts. The large spread in this result can be partially attributed to particles traversing different regions in the vertical cross section of the device and also to the relatively high speed of the particles, which crossed the field of view of the microscope ($\sim$1 mm) after only a few frames of video. Nevertheless, this experiment shows that arrays with triangular posts can operate at significantly higher throughputs for a given pressure drop.

This result agrees with numerical simulations performed on similar array geometries with COMSOL that showed that the average velocity in the array with triangular posts was 82% faster than an array with circular posts for the same pressure gradient. The mechanism behind these findings can be understood qualitatively by drawing an analogy to Poiseuille flow between two parallel plates (White et al. 2006), where the average velocity for a fixed pressure gradient is proportional to the square of distance between plates. Experimentally, the flow rate does not scale exactly as the square of the gap because the confining structure is an array of posts instead of two parallel plates.

3.3 Post shape

Further simulations were performed to explore the effect of post shape on array performance. Figure 5 shows the results of a series of simulations using regular polygons from 3 to 11 sides as the post shape. Arrays with 10-μm post altitude and 10-μm gaps between posts were simulated in COMSOL, and flow profiles across the gap between were extracted for each array. Posts were oriented as shown in the figure inset to examine the difference between having sharp edges on both sides (even number of sides) versus a sharp edge and a flat edge (odd number of sides) on alternate sides of the gap. Critical particle sizes were calculated for tilt angle $\varepsilon = 1/10$ for the top and bottom of the gap and to show the effect of the asymmetric flow profile in posts with an odd number of sides. The critical particle size for circular posts has also been plotted as a dotted line for reference.

The plot shows that a sharp vertex coupled with a flat edge act in unison to produce a smaller critical particle size. The figure shows that sharper vertices reduce the critical particle size. As the number of sides increase, the vertices become less sharp and the critical size increases, approaching that of circular posts. The effect of having a flat edge on the alternate side of the gap is also captured in the figure. In every instance, posts with an odd number of sides have a smaller critical particle size than the even numbered post with one less side, even though its vertices are not as sharp. While the critical size for even numbered posts should be the same for the top and bottom of the gap because of symmetry, the differing geometry across the gap induces an asymmetry in the flow profile that shifts flow toward the bottom half of the gap. Thus, introducing a flat edge opposite a sharp vertex leads to an additional reduction in the critical size. It is when both of these characteristics are combined, as in the case of the equilateral triangle post, that the greatest reduction in critical particle size is seen.

The previous result might lead one to expect that further reduction of the critical particle size might be possible by

using triangular posts with sharper vertices, but additional simulations show that there is a limit to the gains that can be achieved with this approach. Figure 6 shows the results of a series of simulations using triangular posts with varying base width. Arrays with 10-μm post height, 10-μm gaps between posts, and base width between 2 and 40 μm were simulated, and flow profiles across gaps were extracted for each array. Critical particle sizes were calculated for tilt angle $\varepsilon = 1/10$ and plotted as a function of the ratio of the base width to the height of the triangular post. The figure shows that there is an optimal base to height ratio between 1.0 and 1.4 that minimizes the critical particle size to 28% of the gap. Similar to the result with regular polygons, increasing the width of the base beyond 1.4 times the height decreases the sharpness of the vertices and the critical particle size increases. On the other hand, decreasing the base width seems to make it the base act more like a sharp vertex. As the base becomes narrower, the flux shift toward the vertex is reduced as two sides of the gap begin to look the same and the flow profile more closely resembles one of the regular polygons with an even number of sides. Thus, further improvement beyond equilateral triangles by making the post vertices sharper does not seem likely.

3.4 Vertex rounding

The gains achieved by changing the post shape are degraded if care is not taken to maintain sharp post vertices. Figure 7 shows the effect of rounding the post edges on the critical particle size. An array with 10-μm posts, 10-μm gaps between posts, and tilt angle of 1/10 were simulated in COMSOL with the vertices rounded to various radii of curvature ranging from none ($r = 0$) to complete rounding where the final shape is a circle ($r = S/12^{1/2}$). Flow profiles across the gaps were extracted for each rounding, and the critical size for the given tilt was calculated as a percentage of the new gap (10 μm plus the amount of vertex removed to round the vertex). As shown, the critical particle size, starting at 0.28 G when the post is completely triangular, increases 25% to 0.35 G as the post shape transitions from triangular to circular. This transition is a result of the loss of asymmetry in the flow profile that occurs as the vertices become more round. The transition suggests that the post edges should be made as sharp as possible relative to the post side length. Not captured in the figure, but also relevant is the increase in gap size that results from vertex rounding. For a fabrication process that produces a given vertex rounding, it is advisable to use larger posts (increasing S) to decrease r/S and preserve the gains discussed previously and maintain the designed gap size.

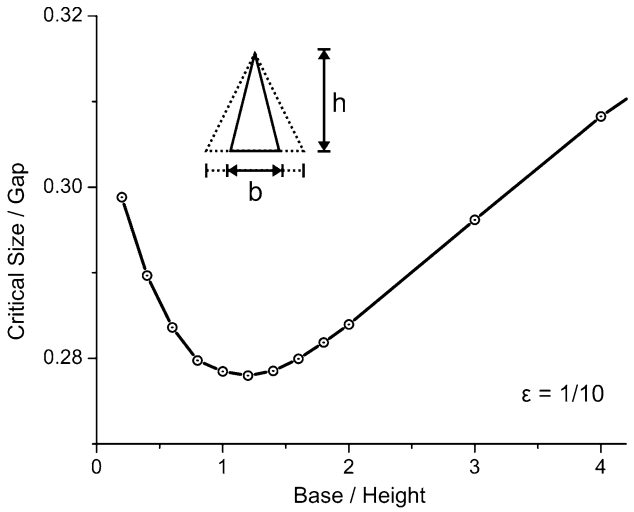

Fig. 6 Critical particle size for arrays of triangular posts with varying base:height ratios. Flow profiles were numerically simulated across gaps between triangular posts in arrays with varying base width. Height of posts and gap between posts was fixed at 10 μm. Critical size for array tilt $\varepsilon = 1/10$ calculated and plotted as a function of ratio of the post base width to height

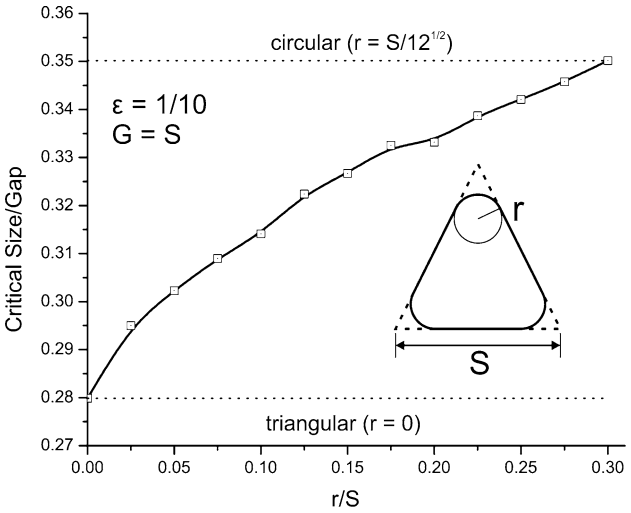

Fig. 7 Effect of vertex rounding on critical particle size as a ratio of the gap. Starting with 10 μm posts with 10 μm gaps, flow profiles across were numerically simulated across gaps between post with no vertex rounding ($r = 0$) to complete vertex rounding ($r = S/12^{1/2}$). Critical size for array tilt $\varepsilon = 1/20$ calculated for resulting gap is plotted as a function of ratio of the rounding to the initial triangle side length

3.5 Post-to-gap ratio

Examining the effect of the post-to-gap ratio on the critical particle size further demonstrates the benefit of using large posts. In circular posts, large posts with small gaps give a more parabolic profile, while small posts with large gaps give a more plug-like profile. Figure 8 shows the effect of

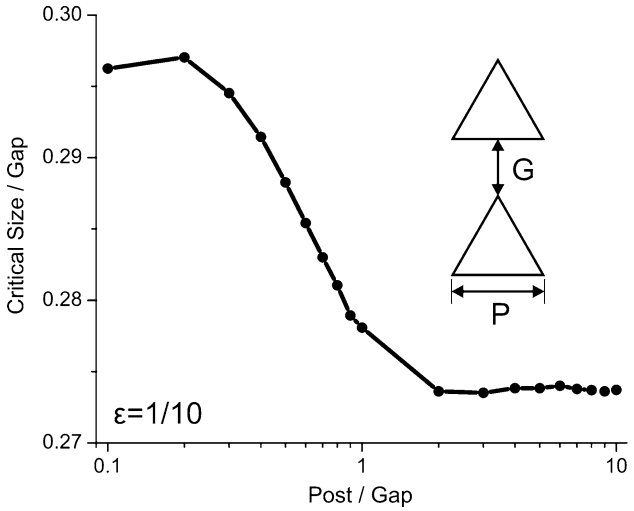

Fig. 8 Critical particle size for arrays of triangular posts with varying post side length to gap ratios. Flow profiles across gaps between triangles were numerically simulated for arrays with varying side length. Gap between posts was fixed at 10 μm. Critical size for array tilt $\varepsilon = 1/10$ calculated and plotted as a function of ratio of the side length to the gap height

changing the post size on the critical particle size. An array with 10-μm gaps between posts and tilt angle of 1/10 was simulated in COMSOL with equilateral triangle posts varying logarithmically from 1 to 100 μm. Flow profiles across the gaps were extracted for each post size, and the critical size for the given tilt was calculated as a percentage of the new. The critical particle size decreases with increasing post size until the post side length is about twice gap and then remains roughly constant for increases in post size thereafter. This transition underscores the effect of the varying post geometry on creating a skewed flow profile also shown in Fig. 6. When the posts are smaller than the gap, they produce a flow profile that is more plug-like and less skewed toward the triangle vertex. It is therefore advisable to make the post side length at least larger than the size of the gap and probably twice the size of the gap to ensure a small critical particle size.

4 Conclusion

We have demonstrated that changing the post shape from circular to triangular in a deterministic lateral displacement device results in a reduced critical particle size as a percentage of the gap. This allows smaller particles to be separated for the same gap and array tilt, larger array tilt for the same critical particle size and gap, and a larger gap for the same critical particle size and array tilt. This last improvement is especially useful as it allows arrays to be designed with a decreased chance of clogging and lower pressure requirement for a desired flow rate. Through a series of simulations, we showed that these gains are accomplished by inducing both a more plug-like flow along the post with a sharp vertex and by producing a shift in flux toward that vertex by having a flat edge on the opposite side of the gap. Of the shapes examined, equilateral triangles provided the greatest reduction in critical particle size and we contend that the future deterministic lateral displacement designs should employ equilateral triangular rather than circular posts.

Acknowledgments This work was supported by award number U54CA143803 from the NCI and HG01506 from the NIH. The content is solely the responsibility of the authors and does not necessarily represent the official views of the National Cancer Institute or the National Institutes of Health. We thank Noah Jafferis for SEM characterization, Clinton Smith and Steve Chou for device etching, and David Inglis for providing circular post bead data.

References

Beech JP, Tegenfeldt JO (2008) Tunable separation in elastomeric microfluidics devices. Lab Chip 8:657–659

Beech JP, Jönsson P, Tegenfeldt JO (2009) Tipping the balance of deterministic lateral displacement devices using dielectrophoresis. Lab Chip 9:2698–2706

Bhagat AAS, Kuntaegowdanahalli SS, Papautsky I (2008) Continuous particle separation in spiral microchannels using Dean flows and differential migration. Lab Chip 8:1906–1914

Davis JA, Inglis DW, Morton KJ et al (2006) Deterministic hydrodynamics: taking blood apart. PNAS 103(40):14779–14784

Di Carlo D, Irimia D, Tompkins RG, Toner M (2007) Continuous inertial focusing, ordering, and separation of particles in microchannels. PNAS 104(48):18892–18897

Huang LR, Cox EC, Austin RH, Sturm JC (2004) Continuous particle separation through deterministic lateral displacement. Science 304:987–990

Inglis DW, Davis JA, Austin RH, Sturm JC (2006) Critical particle size for fractionation by deterministic lateral displacement. Lab Chip 6:655–658

Lindken R, Rossi M, Große S, Westerweel J (2009) Micro-particle image velocimetry (micropiv): recent developments, applications, and guidelines. Lab Chip 9:2551–2567

Loutherback K, Puchalla J, Austin RH, Sturm JC (2009) Deterministic microfluidic ratchet. Phys Rev Lett 102:045301

Lu H, Gaudet S, Schmidt MA, Jensen KF (2004) A microfabricated device for subcellular organelle sorting. Anal Chem 76:5705–5712

Morton KJ, Sturm JC, Austin RH, Chou SY (2006) Proceedings of the μTAS conference 2006, Tokyo, pp 1014–1016

Pamme N (2007) Continuous flow separations in microfluidic devices. Lab Chip 7:1644–1659

Rida A, Gijs MAM (2004) Manipulation of self-assembled structures of magnetic beads for microfluidic mixing and assaying. Anal Chem 76:6239–6246

Squires TM, Quake SR (2005) Microfluidics: fluid physics at the nanoliter scale. Rev Mod Phys 77:977–1026

White FM (2006) Viscous fluid flow, 3rd edn. McGraw Hill, New York, pp 108, 165–171

Yi CQ, Li CW, Ji SL, Yang MS (2006) Microfluidics technology for manipulation and analysis of biological cells. Anal Chim Acta 560:1–23